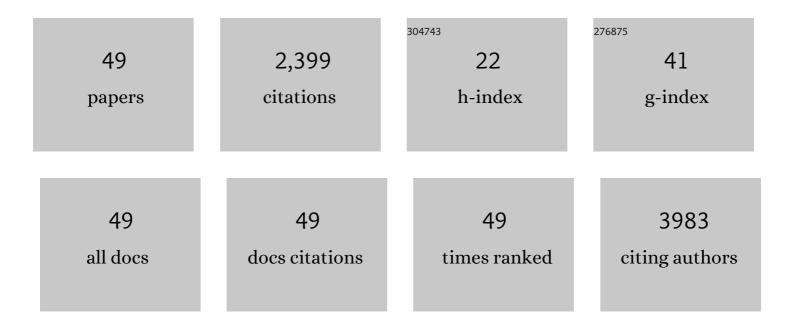
## Liang Li

## List of Publications by Year in descending order

Source: https://exaly.com/author-pdf/10433629/publications.pdf Version: 2024-02-01



LIANCL

#	Article	IF	CITATIONS
1	Temperature-dependent excitonic photoluminescence of hybrid organometal halide perovskite films. Physical Chemistry Chemical Physics, 2014, 16, 22476-22481.	2.8	447
2	Exploration of Crystallization Kinetics in Quasi Two-Dimensional Perovskite and High Performance Solar Cells. Journal of the American Chemical Society, 2018, 140, 459-465.	13.7	327
3	The Additive Coordination Effect on Hybrids Perovskite Crystallization and Highâ€Performance Solar Cell. Advanced Materials, 2016, 28, 9862-9868.	21.0	270
4	Liquid medium annealing for fabricating durable perovskite solar cells with improved reproducibility. Science, 2021, 373, 561-567.	12.6	227
5	Csl Preâ€Intercalation in the Inorganic Framework for Efficient and Stable FA <sub>1â^'</sub> <i><sub>x</sub></i> Cs <i><sub>x</sub></i> Pbl <sub>3</sub> (Cl) Perovskite Solar Cells. Small, 2017, 13, 1700484.	10.0	121
6	A Thermodynamically Favored Crystal Orientation in Mixed Formamidinium/Methylammonium Perovskite for Efficient Solar Cells. Advanced Materials, 2019, 31, e1900390.	21.0	101
7	The Spacer Cations Interplay for Efficient and Stable Layered 2D Perovskite Solar Cells. Advanced Energy Materials, 2020, 10, 1901566.	19.5	89
8	Genetic Correction of Induced Pluripotent Stem Cells From a Deaf Patient With <i>MYO7A</i> Mutation Results in Morphologic and Functional Recovery of the Derived Hair Cell-Like Cells. Stem Cells Translational Medicine, 2016, 5, 561-571.	3.3	67
9	A few-view reweighted sparsity hunting (FRESH) method for CT image reconstruction. Journal of X-Ray Science and Technology, 2013, 21, 161-176.	1.0	60
10	Spectral CT Modeling and Reconstruction With Hybrid Detectors in Dynamic-Threshold-Based Counting and Integrating Modes. IEEE Transactions on Medical Imaging, 2015, 34, 716-728.	8.9	53
11	Unraveling the Growth of Hierarchical Quasi-2D/3D Perovskite and Carrier Dynamics. Journal of Physical Chemistry Letters, 2018, 9, 1124-1132.	4.6	52
12	Precise Composition Tailoring of Mixed-Cation Hybrid Perovskites for Efficient Solar Cells by Mixture Design Methods. ACS Nano, 2017, 11, 8804-8813.	14.6	48
13	A tensor PRISM algorithm for multi-energy CT reconstruction and comparative studies. Journal of X-Ray Science and Technology, 2014, 22, 147-163.	1.0	43
14	Space microgravity drives transdifferentiation of human bone marrowâ€derived mesenchymal stem cells from osteogenesis to adipogenesis. FASEB Journal, 2018, 32, 4444-4458.	0.5	43
15	Differentiation and transplantation of human induced pluripotent stem cell-derived otic epithelial progenitors in mouse cochlea. Stem Cell Research and Therapy, 2018, 9, 230.	5.5	42
16	A general region-of-interest image reconstruction approach with truncated Hilbert transform. Journal of X-Ray Science and Technology, 2009, 17, 135-152.	1.0	36
17	Highâ€Mobility pâ€Type Organic Semiconducting Interlayer Enhancing Efficiency and Stability of Perovskite Solar Cells. Advanced Science, 2017, 4, 1700025.	11.2	36
18	A dynamic material discrimination algorithm for dual MV energy X-ray digital radiography. Applied Radiation and Isotopes, 2016, 114, 188-195.	1.5	29

Liang Li

#	Article	IF	CITATIONS
19	Behavior of stem cells under outerâ€space microgravity and groundâ€based microgravity simulation. Cell Biology International, 2015, 39, 647-656.	3.0	26
20	Induction of differentiation of human embryonic stem cells into functional hair-cell-like cells in the absence of stromal cells. International Journal of Biochemistry and Cell Biology, 2016, 81, 208-222.	2.8	26
21	An amino-substituted perylene diimide polymer for conventional perovskite solar cells. Materials Chemistry Frontiers, 2017, 1, 2078-2084.	5.9	26
22	Effects of simulated microgravity on the expression profiles of RNA during osteogenic differentiation of human bone marrow mesenchymal stem cells. Cell Proliferation, 2019, 52, e12539.	5.3	24
23	Robust multimaterial decomposition of spectral CT using convolutional neural networks. Optical Engineering, 2019, 58, 1.	1.0	23
24	Interior Tomography With Continuous Singular Value Decomposition. IEEE Transactions on Medical Imaging, 2012, 31, 2108-2119.	8.9	18
25	A cone-beam tomography system with a reduced size planar detector: A backprojection-filtration reconstruction algorithm as well as numerical and practical experiments. Applied Radiation and Isotopes, 2007, 65, 1041-1047.	1.5	17
26	A curve-filtered FDK (C-FDK) reconstruction algorithm for circular cone-beam CT. Journal of X-Ray Science and Technology, 2011, 19, 355-371.	1.0	17
27	Experimental measurement of human head motion for high-resolution computed tomography system design. Optical Engineering, 2010, 49, 063201.	1.0	16
28	TRIB3 inhibits proliferation and promotes osteogenesis in hBMSCs by regulating the ERK1/2 signaling pathway. Scientific Reports, 2017, 7, 10342.	3.3	16
29	Dynamic-dual-energy spectral CT for improving multi-material decomposition in image-domain. Physics in Medicine and Biology, 2019, 64, 135006.	3.0	15
30	Identification of stage-specific markers during differentiation of hair cells from mouse inner ear stem cells or progenitor cells in vitro. International Journal of Biochemistry and Cell Biology, 2015, 60, 99-111.	2.8	14
31	Efficient Moistureâ€Resistant Perovskite Solar Cell With Nanostructure Featuring 3D Amine Motif. Solar Rrl, 2018, 2, 1800069.	5.8	13
32	First Dual MeV Energy X-ray CT for Container Inspection: Design, Algorithm, and Preliminary Experimental Results. IEEE Access, 2018, 6, 45534-45542.	4.2	12
33	A curve-based material recognition method in MeV dual-energy X-ray imaging system. Nuclear Science and Techniques/Hewuli, 2016, 27, 1.	3.4	10
34	TRPM7 Upregulate the Activity of SMAD1 through PLC Signaling Way to Promote Osteogenesis of hBMSCs. BioMed Research International, 2020, 2020, 1-23.	1.9	7
35	K-edge eliminated material decomposition method for dual-energy X-ray CT. Applied Radiation and Isotopes, 2017, 127, 231-236.	1.5	6
36	Induction of Functional Hair-Cell-Like Cells from Mouse Cochlear Multipotent Cells. Stem Cells International, 2016, 2016, 1-14.	2.5	5

Liang Li

#	Article	IF	CITATIONS
37	Simultaneous x-ray fluorescence and K-edge CT imaging with photon-counting detectors. Proceedings of SPIE, 2016, , .	0.8	4
38	Edge-oriented dual-dictionary guided enrichment (EDGE) for MRI-CT image reconstruction. Journal of X-Ray Science and Technology, 2016, 24, 161-175.	1.0	3
39	Recent Development of Dual-Dictionary Learning Approach in Medical Image Analysis and Reconstruction. Computational and Mathematical Methods in Medicine, 2015, 2015, 1-9.	1.3	2
40	Dynamic material decomposition method for MeV dual-energy X-ray CT. Applied Radiation and Isotopes, 2018, 140, 55-62.	1.5	2
41	A comparison of projection domain noise reduction methods in low-dose dental CBCT. , 2012, , .		1
42	SIFT-based motion registration for sequence images of instant CT. , 2012, , .		1
43	The simulation of a multi energy bone mineral densitometry method. , 2014, , .		1
44	Material Decomposition of Energy Spectral CT by AUTOMAP. , 2018, , .		1
45	Design of the Multi-Sources Static CT System and its Dual-Energy Monte Carlo Simulation. , 2019, , .		1
46	Establishment of an induced pluripotent stem cell line from a patient with CHARGE syndrome carrying a CHD7 (p.L1151Gfs*17) mutation. Stem Cell Research, 2020, 45, 101774.	0.7	1
47	Without a priori knowledge solving the interior problem in CT using two scans. , 2009, , .		0
48	A Post-Processed Multi-Material Decomposition Method based on Dynamic Dual-energy Detectors. , 2018, , .		0
49	Iterative dynamic dual-energy CT algorithm in reducing statistical noise in multi-energy CT imaging. Physics in Medicine and Biology, 2022, 67, 015003.	3.0	0